

Los Alamos National Laboratory is operated by the University of California for the United States Department of Energy under contract W-7405-ENG-36

LA-UR--85-1347

TITLE: MONTE CARLO ELECTRON/PHOTON TRANSPORT

DE85 010799

AUTHOR(S): Joseph M. Mack, M-4; J. E. Morel, X-6; H. Grady Hughes, X-6

SUBMITTED TO: Joint Los Alamos/CEA Meeting on Monte Carlo Methods, Cadarache, France, April 1985.

DISCLAIMER

This report was prepared as an account of work sponsored by an agency of the United States Government. Neither the United States Government nor any agency thereof, nor any of their employees, makes any warranty, express or implied, or assumes any legal liability or responsibility for the accuracy, completeness, or usefulness of any information, apparatus, product, or process disclosed, or represents that its use would not infringe privately owned rights. Reference herein to any specific commercial product, process, or service by trade name, trademark, manufacturer, or otherwise does not necessarily constitute or imply its endorsement, recommendation, or favoring by the United States Government or any agency thereof. The views and opinions of authors expressed herein do not necessarily state or reflect those of the United States Government or any agency thereof.



By acceptance of this article, the publisher recognizes that the U.S. Government retains a nonexclusive, royalty-free license to publish or reproduce the published form of this contribution or to allow others to do so, for U.S. Government purposes.

The Los Alamos National Laboratory requests that the publisher identify this article as work performed under the auspices of the U.S. Department of Energy

DISTRIBUTION OF THIS DOCUMENT IS UNLIMITED

J.H.

Los Alamos Los Alamos National Laboratory
Los Alamos, New Mexico 87545



MONTE CARLO ELECTRON/PHOTON TRANSPORT

Joseph M. Mack, J. E. Morel, and H. Grady Hughes
Applied Theoretical Physics Division
Los Alamos National Laboratory
Los Alamos, New Mexico

A review of nonplasma coupled electron/photon transport using the Monte Carlo method is presented. Remarks are mainly restricted to linearized formalisms at electron energies from 1 keV to 1000 MeV. Applications involving pulse-height estimation, transport in external magnetic fields, and optical Cerenkov production are discussed to underscore the importance of this branch of computational physics. Advances in electron multigroup cross-section generation is reported, and its impact on future code development assessed. Progress toward the transformation of MCNP into a generalized neutral/charged-particle Monte Carlo code is described.

MONTE CARLO ELECTRON/PHOTON TRANSPORT

INTRODUCTION

The continuing rapid advance of computer technology has dramatically improved the capability of computational physicists to address important problems in applied theoretical physics. One active area of computational physics is simulating coupled electron/photon transport. Space and reactor environments contain electron and photon sources ranging from 1 keV to several tens of MeV (and GeV energies for cosmic rays). The need to detect and control such radiation fields has resulted in a worldwide scientific effort to develop better methods of electron/photon transport. Diagnostic particle physics often focuses on the detection of primary or secondary charged particles. Detector development and design of higher quality diagnostics have provided impetus toward better understanding of electron/photon transport processes. Complex theoretical models must be used to mimic the material interaction of electrons and photons. The added complexity of the electron/photon cascade can result in a computational nightmare that can now be modeled effectively using many commercially available computers.

The basic problem is calculating the transport and penetration of electrons (and their attendant cascades) through matter. Typically, one attempts to solve an appropriate form of a linearized Boltzmann-like equation, for which analytic solutions are generally not available. Numerical methods must be used, and the Monte Carlo method applied to electron/photon transport has become the traditional and most comprehensive approach. Conventional single-scattering Monte Carlo to describe electron Coulombic collisions is prohibitively expensive even on the latest generation computers. This difficulty is effectively circumvented using condensed-history Monte Carlo (CHMC), where multiple-interaction formulas are sampled to obtain a net energy loss and directional change at the end of a macroscopic electron step (path length). Thus, for thousands of collisions along a path length, the cumulative directional and slowing-down effect on an electron trajectory is computed at the path-length end point resulting in enormous time savings. The condensed-history approach provided a breakthrough for doing realistic electron/photon transport problems in many areas of science and engineering.

Treatment of electrons diffusing through matter is only a subset of high-energy (multi-GeV) cascade generation, which includes the "zoo of strange particles." This extremely complex problem is also being simulated using Monte Carlo. As research in high-energy physics grows, simulation of related high-energy cascades will take on a role of increasing importance.

The condensed-history approach requires electron cross sections to be generated in the multiple-interaction context for all relevant interactions.

ELASTIC NUCLEAR OR COULOMB SCATTERING

Nuclear Coulomb scattering is an important interaction mechanism causing electrons to scatter (change direction) with very little energy loss. The long-range Coulomb potential provides the physical basis for the existence of this interaction, and much model development⁹⁻¹¹ has resulted in a comprehensive cross-section data base. Cross sections developed and tabulated by Spencer¹² are valid for a wide range of materials and electron energies.

INELASTIC ELECTRON-ELECTRON SCATTERING

Inelastic electron-electron scattering is generally understood to be the primary energy-loss mechanism for electrons of a few million electron volts. As a result of this interaction, the atomic electrons can find themselves in an excited or ionized state. The ionized state is characterized by a free atomic electron commonly called a delta ray. Excitation of atomic electrons to bound states results in usually negligible soft x-radiation, as the excited electron relaxes to a more stable state. If there is enough energy available, however, an inner-shell electron can be ejected, leaving vacancies deep within the atomic structure. The relaxation of the remaining atomic electrons to a more stable state releases characteristic radiation in the form of x-ray lines at several kiloelectron volts. For some applications, characteristic x rays can be a very important component of the cascade. The theory of Møller¹³ is reliable and widely used to provide cross sections that yield basic stopping-power data, as formulated in the continuous-slowing approximation (CSDA) by Bethe.¹⁴

INELASTIC NUCLEAR SCATTERING

Beyond a few million electron volts, another energy-loss mechanism usually dominates, that being inelastic nuclear scattering, which results in bremsstrahlung production. The basic process involves an inelastic free electron-nucleus collision accompanied by the emission of an appropriate quanta of radiation. The theory of Bethe and Heitler¹⁵ is commonly used to provide a data base for cross sections describing inelastic nuclear scattering, but the most comprehensive review of the subject is given by Koch and Motz.⁷

ELECTRON MULTIPLE INTERACTIONS

As an electron traverses a small fraction of its range, it undergoes an enormously large number of interactions of the aforementioned types. Because of this approximately continuous behavior, it is possible to describe the net or cumulative effect of these interactions on the electron trajectory by applying multiple-interaction theories to phenomena associated with electron energy loss and directional changes.

The continuous slowing-down approximation of Bethe¹⁴ (CSDA) is often used to construct collisional stopping powers for electrons in various media. Generally, stopping powers describe the average energy loss that an electron experiences upon moving a prescribed distance (path length). Stopping powers based on collisional energy loss due to inelastic electron-electron scattering were later modified by Rohrlich and Carlson¹⁶ to include the effects of energy loss from bremsstrahlung production--the so-called radiative stopping power. The total stopping power of an electron in a given material is composed of a collisional and radiative component that establishes the average energy loss

These include elastic nuclear scattering, inelastic atomic electron scattering, and the production of secondary photons (for example, annihilation quanta, fluorescence, and bremsstrahlung). The means exist for computing all the required random-walk cross sections in a continuous-energy framework; however, the interaction physics is currently in need of overhaul. As the need for electron-transport simulation rises, increased motivation for improving the cross-section generators will result.

Ideas mentioned previously have been evolving since the early 1960's and are at a sophisticated stage of development and usefulness. There are interesting new directions under investigation that will lead to even more flexible problem-solving capability. Continuous-energy electron Monte Carlo has been the traditional method, but there is a significant, relatively new effort toward generating multigroup electron cross sections. Not only will the multigroup formalism yield increased computational speed for many problems but also will facilitate the development of an adjoint electron/photon transport capability. Often electrons transport through matter under the influence of externally imposed or self-consistent electromagnetic fields. Transport of electrons in external magnetic fields is currently being treated with generality; the non-linear problem of electron transport within self-consistent fields is in the research stage. Merging electron Monte Carlo transport physics to a self-consistent field, particle-in-cell approach is currently under investigation.

Prior knowledge of photon-interaction physics is assumed; however, relevant physics of electron-material interactions is mentioned for continuity. The essential ideas of CHMC are presented along with important applications. Future directions including multigroup electron transport, adjoint approaches, and generalized neutral/charged-particle version of MCNP are indicated.

ELECTRON PHYSICS

Extensive reviews of electron physics are presented elsewhere;¹⁻³ however, a synopsis of relevant electron processes is given. Whereas photon interaction is not presented, the strong coupling that can exist between electron and photon fields in cascade is of fundamental importance.

The passage of high-energy electrons through matter involves a number of interactions such as elastic nuclear scattering, inelastic atomic electron scattering, inelastic nuclear scattering, and the production of secondary photons (for example, fluorescence and bremsstrahlung). Of course, the photons can further produce secondary electrons by photoelectric, Compton, and pair-production processes. The repetition of this cycle ultimately results in an electron/photon cascade. At high energies, electron/photon coupling is quite strong but very forward peaked, thus allowing some simplifying approximations, particularly as regards the angular distributions required. As electrons assume lower energies, the coupling becomes weaker, but the required peculiarity found in coupled electron/photon transport is that the cascade can carry substantial amounts of primary electron energy to spatial locations at much greater than the primary electron ranges as a consequence of the diverse relative mean-free paths for electrons and photons. The solutions to many practical problems lie in the ability of the computational physicist to ascertain the type and nature of dominant processes.

of the electron per unit path length. There is, however, an added complexity in that some electrons lose substantially more energy than the average, as defined by the CSDA model. Such a deviation from the CSDA average energy loss is termed the energy-straggling problem.¹⁷ Through the efforts of Landau¹⁸ and Blunck and Westphal¹⁹ a energy-loss distribution function has been established that includes broadening (or straggling) due to both collisional and radiative energy losses.

As electrons diffuse in matter, energy is lost and energy straggling is possible; analogously, they also suffer many small-angle deflections, and angular straggling can also occur. A number of multiple-scattering theories exist, but most of them suffer from compromise in an attempt to treat small- and large-angle scattering, as well as lateral displacement. Palatable reviews of this subject are found in Thompson³ and Zerby.⁶ The optimal approach for accurately describing all important aspects of multiple scattering is a controversial subject. In general, electron-interactions cross sections are reviewed and improved in rather piecemeal fashion. For details on the current status of such data, refer to papers by Peek,⁸ Seltzer and Berger,²⁰ Berger and Seltzer,²¹ Scott,²² and Devaney.²³

The National Bureau of Standards, under the leadership of Martin J. Berger, has developed into a single package the most comprehensive computational models of the aforementioned electron physics. This package, under the generic name DATPAC,²⁴ is available worldwide from the Radiation Information Shielding Center (RSIC), Oak Ridge National Laboratory, Oak Ridge, Tennessee, USA. Cross sections produced by DATPAC are tabulated on a preselected set of logarithmically spaced electron-energy grid points, which can be accurately interpolated to intermediate energies.

CONDENSED-HISTORY MONTE CARLO

The problem of simulating the transport of electrons in matter basically is one of solving an appropriate transport equation. The transport of electrons is, in some respects, similar to that of neutrons. Through a variety of interactions (mentioned in the previous section), electrons experience a slowing-down process and the production of various components of secondary radiation, such as bremsstrahlung and knock-on electrons. The primary distinction from neutron transport is a consequence of charge and its manifestation in the form of long-range Coulombic interactions, including small and large energy/angle changes. Many thousands more collisions are required for an electron to slow down to a given energy than for a neutron at similar initial energy. The important effects of charge must be included in the transport formalism.

The transport equation in its linearized form is taken from Berger.²⁵

$$\frac{1}{v} \frac{\partial \phi(E, \vec{r}, \vec{\Omega}, t)}{\partial t} + \vec{\Omega} \cdot \nabla \phi(E, \vec{r}, \vec{\Omega}, t) + \sum_a (E) \phi(E, \vec{r}, \vec{\Omega}, t) = \int_E^\infty dE' \int_{4\pi} \phi(E', \vec{\Omega}', \vec{r}, t) K(E' + E, \vec{\Omega}' + \vec{\Omega}) d\vec{\Omega}' \quad , \quad (1)$$

where

t = time,
 v = particle speed,
 E = electron energy,
 \vec{r} = electron spatial vector,
 $\vec{\Omega}$ = electron direction vector,

$\phi(E, \vec{r}, \vec{\Omega}, t) dE d\vec{\Omega}$ = particle flux at t, r in intervals $(E, E + dE)$, $(\vec{r}, \vec{\Omega} + d\vec{\Omega})$,

$\Sigma_a(E)$ = interaction probability per unit path length, and

$K(E' \rightarrow E, \vec{\Omega}' \rightarrow \vec{\Omega}) dE d\vec{\Omega}$ = probability per unit path length that a particle at $E', \vec{\Omega}'$ after collision will move to the interval $(E, E + dE)$, $(\vec{\Omega}, \vec{\Omega} + d\vec{\Omega})$.

Equation (1) is the usual description of a collision-by-collision phase-space balancing. The first term on the left-hand side represents the time-rate-of-change of flux; the second, leakage; and the third, interaction losses. The right-hand side indicates the phase-space scattering or collision balance.

In principle, single-scattering Monte Carlo can be used to solve Eq. (1) in integral form. This is accomplished by tracking electrons from collision to collision and can be illustrated by the following collision array

$$\begin{array}{l}
 E_0, E_1, E_2, \dots, E_n, \dots \\
 \vec{\Omega}_0, \vec{\Omega}_1, \vec{\Omega}_2, \dots, \vec{\Omega}_n, \dots \\
 \vec{r}_0, \vec{r}_1, \vec{r}_2, \dots, \vec{r}_n, \dots,
 \end{array} \tag{2}$$

where $E_n, \vec{\Omega}_n, \vec{r}_n$ are the energy, direction, and position of the particle at the n th collision location. The transport equation defines the probabilities of phase-space transitions from one column to the next.

This single-scattering approach is effective when dealing with neutral particles (for example, neutrons and photons) whose mean-free paths are relatively long. Long-range Coulombic interactions cause electrons to experience an enormous number of collisions while traversing an equivalent mean-free path of a neutron or photon. For example, on average, about 18 collisions of a neutron in hydrogen will reduce its energy from 2 MeV to thermal; whereas, an electron requires many thousands of collisions for equivalent energy loss. Therefore, simulation of explicit electron collisions, even on modern high-speed computers, is impractical in terms of time and cost.

CHMC,²⁵ as developed by Berger, provides the necessary breakthrough for circumventing this difficulty. Essentially, CHMC accounts for the cumulative effect on electron trajectories of numerous collisions along a macroscopic path length (small fraction of an electron range). Thus, we include the path length, S , in the collision-array description (Eq. 2),

$$\begin{aligned}
& 0, S_1, S_2, \dots, S_n \dots \\
& E_0, E_1, E_2, \dots, E_n \dots \\
& \vec{\Omega}_0, \vec{\Omega}_1, \vec{\Omega}_2, \dots, \vec{\Omega}_n \dots \\
& \vec{r}_0, \vec{r}_1, \vec{r}_2, \dots, \vec{r}_n \dots,
\end{aligned} \tag{3}$$

where E_n , $\vec{\Omega}_n$, \vec{r}_n are the electron energy, direction, and position after traversing a macroscopic path length S_n . Particle transition from column n to column $n + 1$ is defined by Monte Carlo sampling of appropriate multiple-interaction theories, which are formulated in terms of path length. Because of these considerations and noting that path length is the time integral of velocity and electron energy, E , is related to the path length, S , by the stopping power dE/dS , the transport operation (Eq. 1) can be put in terms of path length. Zerby and Moran²⁶ and Berger²⁷ were the first to successfully implement the condensed-history scheme into a usable code framework in the early 1960's. Berger concentrated on cross-section generation as applied to one-dimensional CHMC. Using essentially the same physics cross sections, others²⁸⁻³² extended the dimensionality of the random walk to three-dimensional generalized geometry.

SIGNIFICANT APPLICATIONS

There are numerous applications that use coupled electron/photon Monte Carlo transport codes. We choose to concentrate on three: (1) pulse-height tallies, (2) simulation of gas Cerenkov detectors, and (3) magnetic-spectrometer design. These items serve to establish the versatility and general usefulness of the method, particularly in terms of diagnostic development.

PULSE-HEIGHT ANALYSIS

Electron CHMC coupled to photon single-scattering particle tracking provides a detailed energy-loss record of all cascade particles. We take advantage of this by noting direct similarity to the energy-loss accounting scheme of multichannel analyzers (MCA). MCAs count the number of source particles that lose specific amounts of energy, ΔE , within an active detector region. The Monte Carlo analogy to MCA particle counting is tallying weight in appropriate energy-loss bins. The Monte Carlo tally actually defines the spectrum of absorbed energy, which is converted to pulse-height spectrum by folding with the instrument response. Obviously, such information is ideally suited for investigations of detector efficiency and response.

We present one typical example of such a Monte Carlo simulation as it compares to experiment. A bismuth germanite (BGO) scintillator geometry, bombarded by a ¹³⁷Cs photon source, is shown in Fig. 1. The geometry is cylindrically symmetric about the "dashed line." The 7.6-cm by 7.6-cm BGO crystal has an aluminum case (0.05-cm thick) surrounding the front and lateral sides of the crystal cylinder. Internal to the aluminum at the front of the detector are layers of sponge rubber and polyethylene (0.1-cm thick) that we have assumed to be 100% polyethylene. Finally, there is also a magnesium oxide reflector (0.2-cm thick) adjacent to the front end and lateral sides of the crystal.

Also indicated in Fig. 1 is a point isotropic source at some representative distance from the front face of the detector. Pulse-height distributions were calculated at different source-to-detector distances. The photomultiplier tube is shown for completeness; however, because it contributes less than 20% to the 180° backscatter, it was not explicitly modeled in the Monte Carlo simulations. Similarly, the concrete walls of the room in which the empirical data were acquired were not included in the Monte Carlo simulations. The pulse-height spectrum was measured and computed (with Monte Carlo) by Hsu³³ et al., and the results compared in Fig. 2. We find excellent agreement ($\pm 3\%$) at the photopeak and Compton edge, and quite respectable correlation exists over the entire energy range. The discrepancy between computation and experiment in the 0.6- to 0.65-MeV region is a consequence of instrumental broadening in the measurement and poor statistics in the Monte Carlo. Clearly, the pulse-height tally yields an accurate computational means to investigate BGO detector design. Furthermore, it is natural and correct to extend this conclusion to an impressive variety of other detector designs.

CERENKOV RADIATION

Recently, the production and generalized ray trace of Cerenkov radiation has been implemented^{34,35} in the three-dimensional member of the Integrated Tiger Series (ITS) code package.³² Once again, the condensed-history approach is used to generate Cerenkov along a path length. Directionality is given by the Cerenkov relation

$$\cos \theta = \frac{1}{\beta n(\lambda)} \quad , \quad (4)$$

where β is the ratio of electron speed in the medium to the speed of light in vacuum, n is the material refractive index at wavelength λ , and θ the Cerenkov-emission angle relative to the electron direction. Cerenkov photon number production along a path length is given by

$$\frac{dN}{dS} = 2\pi\alpha \int_{\lambda_1}^{\lambda_2} \left\{ 1 - \frac{1}{\beta^2 n^2(\lambda)} \right\} \frac{d\lambda}{\lambda^2} \quad , \quad (\lambda_2 > \lambda_1) \quad , \quad (5)$$

where α is the fine-structure constant.

Cerenkov production coupled to detailed Monte Carlo electron/photon transport yields a powerful tool in the study of Cerenkov-detection schemes useful in many areas of physics. In the new model, once a Cerenkov photon is generated, a photon ray trace is activated; the Cerenkov photon is then followed throughout the general 3-D geometry. Each Monte Carlo cell has an associated set of bulk optical properties, which act as boundary conditions as the photon reaches a given cell. These properties include refractive index (Snell's law), specular and diffuse reflection, and extinction and transmission coefficients. With these zonal bulk properties Cerenkov production and complex optical-system analysis can proceed on line during the Monte Carlo simulation. A typical example³⁵ of a CO₂ gas Cerenkov detector studied using the new model is illustrated in Fig. 3. Threshold-production curve computations for this geometry are plotted in Fig. 4. The behavior of the production (Fig. 4) is anticipated through Eq. (5) in that a sharp production increase is found near the threshold energy followed by saturation, as the beam energy is increased.

The lower curve indicates the number of Cerenkov photons reaching the detector (through optics) for each produced within the gas volume--hence the overall system efficiency. This example illustrates the power of incorporating other specific cascade components into the general simulation scheme.

TRANSPORT IN EXTERNAL MAGNETIC FIELDS

The capability to treat electron transport under the influence of externally imposed, spatially general magnetic fields now exists in the ITS package.¹⁶ This model utilizes all of the previously mentioned electron physics in the condensed-history framework. The effect on the electron trajectory of the magnetic field along a macroscopic path length is computed by numerical integration of equations of motion (in vacuum) as derived from the relativistic Lorentz-force equation:

$$F = m_{\gamma} \frac{d\vec{v}}{dt} = q[\vec{E} + \vec{v} \times \vec{B}] \quad (6)$$

The magnetic field, electric field, and charge are given by \vec{B} , \vec{E} , and q , respectively. The mass, m_{γ} , in Eq. (8) is the relativistic mass. Transport in magnetic fields involves directional changes only, which are superimposed on the collisional effects of electron direction at the end of each macroscopic path length; whereas, electric fields produce directional and energy changes.

There are many important applications including bremsstrahlung-converter optimization¹⁷ and magnetic-spectrometer design. The graphical results of a Monte Carlo spectrometer simulation¹⁸ are shown in Fig. 5. Two-dimensional projections of three secondary electron trajectories (14-17 MeV) are plotted as they leave the lead converter foil and move through an inhomogeneous \vec{B} -field region shown by the rings in Fig. 5. The curvature of the trajectories is dependent on the \vec{B} -field intensity variation, where the intensity increases from outer to inner rings. Because of the \vec{B} -field strength, electrons turn through 180° to intersect the A-A plane. This interaction point thus defines a spectrometer-detector channel location for 14- to 17-MeV energies. Similarly, other energy-channel detector locations can be defined, and the spectrometer design optimized.

NEW DIRECTIONS

Approximately 30 years have elapsed in the development of computational methods for electron/photon transport. The field has reached a juncture where new trends may raise it to greater levels of problem-solving capability. It is entertaining and beneficial to contemplate some future possibilities--particularly that of a new method involving multigroup electron cross sections.

HYBRID MULTIGROUP/CONTINUOUS-ENERGY ELECTRON/PHOTON MONTE CARLO

The CHMC method is a continuous-energy method used in essentially all production-coupled electron/photon transport codes.^{27, 28} Continuous-energy methods are accurate for forward calculations, but they are not easily applied to adjoint calculations. It is probably for this reason that a production capability for continuous-energy coupled electron/photon adjoint transport calculations has been difficult to realize.

Unlike continuous-energy methods, the multigroup Monte Carlo method is easily applied to adjoint calculations. For instance, production multigroup Monte Carlo codes can perform both forward and adjoint calculations with the same cross-section input.³ Such a dual capability is obviously very powerful. The multigroup method is known to give adequate engineering accuracy for photon-transport calculations, but the accuracy of this method for electron-transport calculations is still being explored. In general, the multigroup method is only appropriate for treating energy losses that are greater than or equal to the average width of a group. When traveling through matter, an electron (on the average) has an enormous number of Coulombic interactions in which only a very small fraction of its energy is lost. These "small" energy losses are far too minute to be resolved with a reasonable number of groups. One possible approach for circumventing this difficulty is to use a Fokker-Planck operator⁴ to model the "small" energy losses while retaining the full Boltzmann description for the "large" energy transfers. The central idea of this hybrid Boltzmann-Fokker-Planck approach is that the multigroup method is only used to treat those transfers that can be adequately resolved with a reasonable number of groups. A rigorous simulation of the Fokker-Planck operator requires a continuous-energy treatment, but the standard multigroup method assigns only a discrete energy group index to each particle. This index does not correspond to a unique energy, but rather a continuum of possible energies within the group. If a rigorous simulation of the Fokker-Planck operator is to be performed in conjunction with a multigroup treatment for the Boltzmann operator, the multigroup method must be modified to accommodate particles with continuously varying energies. The purpose of this discussion is to propose such a method.

The central idea of our approach can be demonstrated in terms of the following hybrid Boltzmann-Fokker-Planck transport equation:

$$\mu \frac{\partial \psi}{\partial z} + \sigma_t \psi = \int_0^{\infty} \int_{-1}^{+1} \sigma_s(E' \rightarrow E, \mu_0) \psi(\mu', E') d\mu' d\phi' dE' + \frac{\partial [\xi \psi]}{\partial E} \quad (7a)$$

where

$$\mu_0 = \mu' \mu - [(1 - \mu'^2)(1 - \mu^2)]^{1/2} \cos(\phi') \quad , \quad (7b)$$

μ denotes the cosine of the polar angle defining the particle direction with respect to the z-axis, E denotes the particle energy, ψ denotes the angular flux, σ_t denotes the total cross section, $\sigma_s(E' \rightarrow E, \mu_0)$ denotes the scattering cross-section differential in final energy and scattering cosine, and ξ denotes the stopping power. Equation (7) is a hybrid equation because it contains both the continuous-slowning-down Fokker-Planck operator¹ and the standard Boltzmann-scattering operator. Our hybrid multigroup-continuous-energy algorithm for solving Eq. (7) follow directly from two assumptions. First, we assume that the cosine dependence in the scattering cross section can be expressed in terms of a Legendre polynomial expansion. Second, we assume that the energy dependencies of the cross sections and stopping power appearing in Eq. (7) can be approximated with piecewise-constant basis functions. In particular, we first use a standard Legendre polynomial cosine expansion for the scattering cross section:

$$\tilde{\sigma}_S(E' \rightarrow E', \mu_0) = \sum_{\ell=0}^L \frac{(2\ell + 1)}{4\pi} \sigma_S^\ell(E' \rightarrow E) P_\ell(\mu_0) \quad , \quad (8a)$$

where

$$\sigma_S^\ell(E' \rightarrow E) = 2\pi \int_{-1}^{+1} \sigma_S(E' \rightarrow E, \mu_0) P_\ell(\mu_0) d\mu_0 \quad , \quad \ell = 0, L \quad , \quad (8b)$$

$P_\ell(\mu_0)$ denotes the Legendre polynomial of degree ℓ , and L denotes the degree of the expansion. Next we partition the energy domain into a total of G contiguous intervals or "groups." The g 'th group has an upper boundary energy $E_{g-1/2}$, a midpoint energy E_g , and a lower boundary energy $E_{g+1/2}$. A corresponding set of piecewise-constant basis functions is defined as follows:

$$B_g(E) = 1.0 \quad , \quad \text{if } E_{g-1/2} > E \geq E_{g+1/2} \quad , \quad (9)$$

$$= 0.0 \quad , \quad \text{otherwise} \quad .$$

Defining the energy-expansion coefficients to obtain integral weighted-least-square fits, we obtain:

$$\tilde{\sigma}_t(E) = \sum_{g=1}^G \sigma_{t,g} B_g(E) \quad , \quad (10a)$$

$$\sigma_{t,g} = \left[\int_{\Delta E_g} \sigma_t(E) W_g(E) dE \right] / \Delta E_g \quad , \quad (10b)$$

$$\xi(E) = \sum_{g=1}^G \xi_g B_g(E) \quad , \quad (11a)$$

$$\xi_g = \left[\int_{\Delta E_g} \xi(E) W_g(E) dE \right] / \Delta E_g \quad , \quad (11b)$$

$$\tilde{\sigma}_S(E' \rightarrow E, \mu_0) = \sum_{g=1}^G \sum_{k=1}^G \sum_{\ell=0}^L \frac{(2\ell + 1)}{4\pi \Delta E_g} \sigma_{S,k+g}^\ell P_\ell(\mu_0) B_k(E') B_g(E) \quad , \quad (12a)$$

$$\sigma_{S,k+g}^\ell = \left[\int_{\Delta E_g} \int_{\Delta E_k} \sigma_S^\ell(E' \rightarrow E) W_k(E') W_g(E) dE' dE \right] / \Delta E_k \quad , \quad (12b)$$

where $W_g(e)$ denotes an arbitrary normalized weight function for the g 'th

energy interval, and $\Delta E_g = E_{g-1/2} - E_{g+1/2}$. Substituting these expansions into Eq. (7), we obtain an approximate equation that becomes equivalent to Eq. (7) in the limit as the Legendre expansion degree is increased, and the group widths are decreased:

$$\mu \frac{\partial \psi}{\partial z} + \tilde{\sigma}_t \psi = \int_0^\infty \int_0^{2\pi} \int_0^{\pi} \tilde{\sigma}_s(E' \rightarrow E, \mu_0) \psi(\mu', E') d\mu' d\phi' dE' + \frac{\partial[\xi\psi]}{\partial E} \quad (13)$$

It is straightforward to develop a Monte Carlo algorithm for rigorously solving Eq. (13), which is independent of the particular values of the expansion coefficients. In principle, one could use this approach to solve a wide variety of transport problems by supplying the expansion coefficients appropriate to the problem of interest (that is, for neutrons, coupled electrons and photons, etc.). The versatility of the standard multigroup method is retained. Although this approach is a continuous-energy method for an approximate equation, we refer to it as a hybrid multigroup-continuous-energy method because it is closely related to the standard multigroup method. To demonstrate this, we integrate Eq. (13) over all energies:

$$\begin{aligned} \mu \frac{\partial \psi_g}{\partial z} + \sigma_{t,g} \psi_g &= \sum_{k=1}^G \sum_{l=0}^L \frac{(2l+1)}{4\pi} \sigma_{k \rightarrow g}^l \phi_k^l P_l(\mu) \\ &+ \xi_{g-1} \psi_{g-1/2} - \xi_{g+1/2} \psi_{g+1/2}, \quad g = 1, G \end{aligned} \quad (14a)$$

where

$$\psi_g = \int_{\Delta E_g} \psi_g dE, \quad (14b)$$

$$\phi_g^l = 2\pi \int_{-1}^{+1} \psi_g(\mu_0) P_l(\mu_0) d\mu_0. \quad (14c)$$

Although our expansion coefficients were derived to provide piecewise-constant fits in the energy variable for the cross sections and stopping power, they are identical to the standard multigroup-Legendre coefficients generated with the weight functions used in the fits. Thus, if the stopping power is zero for all groups, Eq. (14) is rigorously equivalent to the standard Boltzmann-multigroup approximation to Eq. (7). This means that our method can be used to provide standard Boltzmann-multigroup solutions in addition to Boltzmann-Fokker-Planck solutions. Furthermore, standard multigroup cross-section data can be used in both types of calculations, and our method represents a generalization rather than a variation of the standard multigroup method.

The adjoint of Eq. (13) is

$$\begin{aligned}
-\mu \frac{\partial \psi^\dagger}{\partial z} + \tilde{\sigma} \psi^\dagger &= \int_0^\infty \int_0^{2\pi} \int_{-1}^{+1} \tilde{\sigma}_s(E \rightarrow E', \mu \rightarrow \mu') \psi^\dagger(\mu', E') d\mu' d\phi' dE' \\
&+ \frac{\partial \tilde{\xi} \psi^\dagger}{\partial E} - \frac{\partial [\tilde{\xi} \psi^\dagger]}{\partial E} .
\end{aligned} \tag{15}$$

The Monte Carlo algorithm for solving Eq. (15) differs only slightly from that for solving Eq. (13) in that adjunctions (adjoint particles) may be created or destroyed in both the scattering and slowing-down processes. One can, however, devise a generalized Monte Carlo algorithm for solving both Eqs. (7) and (9) using the same expansion coefficients previously defined. As a result, our hybrid scheme retains the powerful adjoint capability associated with the standard-multigroup method. We know of only one serious attempt at modeling the adjoint of the electron-transport equation. The NOVICE code² simulates the adjoint electron/bremsstrahlung process in a continuous electron energy format. Comparisons are currently underway between NOVICE and ITS for selected problems; the results³ will be published in the open literature by mid-1985.

We intend to computationally test our multigroup approach for solving both forward and adjoint coupled electron/photon transport problems. Considering recent results regarding the accuracy of the multigroup/discrete-ordinates method for coupled electron/photon transport,⁴ we fully expect that our hybrid multigroup-continuous-energy Monte Carlo algorithm will be adequate for our purposes.

GENERAL PARTICLE CODE

The need to simulate systems consisting of many types of neutral and charged particles is increasing. This originates primarily from diverse current and future applications in many branches of physics. Manageability of a number of simulation codes, each to treat specific particle coupling, becomes a Herculean task. (In fact, motivation for combining various electron/photon codes into one ITS package stems from the management difficulties of eight separate codes.) Thus, the drive to develop a general-particle Monte Carlo transport code appears justified.

The transformation of the MCNP code into a general-particle code is in progress. The initial task is to implement electrons into MCNP, with a further plan to merge the high-energy cascade particles, as treated in the HETC⁵ code. A procedure of particle flagging will be established to allow the user to be selective in cascade characterization. Improved manageability of the general-particle code will promote more efficient maintenance, clearer code-development directions, better code portability, and higher quality documentation.

MISCELLANEOUS

The versatility and success of Monte Carlo techniques in simulating relativistic electron/photon transport have generated the intriguing possibility of including macroscopic and self-consistent electric and magnetic fields in multidimensional geometry. External field calculations have already been mentioned with some success using Monte Carlo^{6,7} and discrete-ordinates;⁸

self-consistent fields have been included in simple geometry.⁶ Of course, the ultimate goal is to obtain a good self-consistent field in a 3-D Monte Carlo framework. One likely possibility is coupling Monte Carlo simulation to a particle-in-cell structure. As electron/photon electromagnetic-field codes evolve, many new computational challenges will be exposed that, once met, shall provide a means to address other important classes of problems, heretofore inaccessible.

To reduce the time devoted to electron-collision tracking, multiple-interaction theories are usually implemented. Therefore, a variety of variance-reduction techniques are needed that reflect the context of CHMC. Further most of the codes in use adequately address primarily only one energy regime; serious attempts should be made to extend the energy coverage, both to higher and lower energies.

In summary, the discipline of computational electron/photon transport-methods development is and will be enjoying incredible stimulation. The outcome of such activity is predictable: substantial progress will be forthcoming that will greatly extend our understanding of basic transport processes, and our capability will be improved to meet new challenges in diagnostic physics and radiation protection.

REFERENCES

- ¹ R. D. Birkhoff, Handbuch der Physik, S. Flugge, Ed. (Springer-Verlag, Berlin, 1958), Vol XXXIV.
- ² R. D. Evans, The Atomic Nucleus (McGraw-Hill Book Co., New York, 1955).
- ³ W. L. Thompson, "Gamma-Ray and Electron Transport," Ph.D. thesis, University of Virginia (Charlottesville, Virginia, 1974).
- ⁴ James M. Peek, "Cross-sections for Electron and Photon Processes Required by Electron-Transport Calculations," Sandia National Laboratories report SAND 79-0772 (Albuquerque, New Mexico, November 1979).
- ⁵ B. Rossi, High Energy Particles (Prentice-Hall, Englewood Cliffs, New Jersey, 1952).
- ⁶ H. A. Bethe and J. Ashkin, "Passage of Radiation Through Matter," Experimental Nuclear Physics, E. Segre, Ed. (John Wiley and Sons, Inc., New York, 1953), Vol. I.
- ⁷ H. W. Koch and J. W. Motz, "Bremsstrahlung Cross-Section Formulas and Related Data," Rev. Mod. Phys. 31, 920 (1959).
- ⁸ C. D. Zerby and F. L. Keller, "Electron Transport Theory and Experiments," Nucl. Sci. and Eng. 27, 190 (1967).
- ⁹ N. F. Mott, "The Scattering of Fast Electrons by Atomic Nuclei," Proc. Roy. Soc. London A124, 425 (1929).
- ¹⁰ G. A. Goudsmit and J. L. Saunderson, "Multiple Scattering of Electrons," Phys. Rev. 57, 24 (1940).

- ¹¹ G. Mollere, "Theorie der Streuung schneller geladener Teilchen I," Z. Naturforschung 2a, 133 (1947).
- ¹² L. V. Spencer, "Energy Dissipation by Fast Electrons," NBS Monograph 1, National Bureau of Standards (U.S. Department of Commerce, Washington, D.C., 1959).
- ¹³ C. Møller, "Zur Theorie des Durchgangs schneller Elektronen durch Materie," Ann. Physik 14, 531 (1932).
- ¹⁴ H. A. Bethe, "Quantenmechanik der Ein- und Zwei-Elektronen-Problemen," Handbuch der Physik, H. Geiger and Karl Scheel, Eds. (Julius Springer, Berlin, 1933), Vol. XXIV/1.
- ¹⁵ H. A. Bethe and W. Heitler, "On Stopping of Fast Particles and on the Creation of Positive Electrons," Proc. Roy. Soc. London A146, 83 (1934).
- ¹⁶ F. Rohrlich and B. C. Carlson, "Positron-Electron Differences in Energy-loss and Multiple Scattering," Phys. Rev. 93, 38 (1954).
- ¹⁷ E. J. Williams, "The Straggling of β Particles," Proc. Roy. Soc. London A125, 420 (1929).
- ¹⁸ L. Landau, "On the Energy Loss of Fast Particles by Ionization," J. Phys. USSR 8, 201 (1944).
- ¹⁹ O. Blunck and K. Westphal, "Elektronen in dünnen Schichten," Z. Physik 130, 641 (1951).
- ²⁰ S. M. Seltzer and M. J. Berger, "Status of Electron Transport Cross Sections," National Bureau of Standards report NBSIR 82-2572 (U.S. Department of Commerce, Washington, D.C., September 1982).
- ²¹ M. J. Berger and S. M. Seltzer, "Stopping Power and Ranges of Electrons and Positrons," National Bureau of Standards report NBSIR 82-2550 (U.S. Department of Commerce, Washington, D.C., August 1982).
- ²² W. T. Scott, "The Theory of Small-Angle Multiple Scattering of Fast Charged Particles," Rev. Mod. Phys., 231 (1963).
- ²³ Joseph J. Devaney, "Electron Multiple, Plural, and Single Scattering," Los Alamos National Laboratory report LA-10272-MS (Los Alamos, New Mexico, March 1985).
- ²⁴ M. J. Berger and S. M. Seltzer, "Electron and Photon Transport Programs," Part I, "Introduction and Notes on Program DATAPAC 4," National Bureau of Standards report NBS-9836 (U.S. Department of Commerce, Washington, D.C., June 1968).
- ²⁵ M. J. Berger, "Monte Carlo Calculations of the Deep Penetration and Diffusion of Fast Charged Particles," Methods in Computational Physics, B. Adler, S. Fernbach, and M. Rotendry, Eds. (Academic Press, New York, 1963), Vol. I.

- 26 C. D. Zerby and H. S. Moran, "A Monte Carlo Calculation of the Three-Dimensional Development of High-Energy Electron-Photon Cascade Showers," Oak Ridge National Laboratory report ORNL-TM-422 (Oak Ridge, Tennessee, 1962).
- 27 M. J. Berger and S. M. Seltzer, "ETRAN Monte Carlo Code System for Electron and Photon Transport Through Extended Media," Oak Ridge National Laboratory report CCC-107 (Oak Ridge, Tennessee, 1968).
- 28 T. M. Jordan, "BETA-II: A Time-Dependent, Generalized Geometry Monte Carlo Program for Bremsstrahlung and Electron Transport Analysis," Applied Research Technology Corporation report ART-60 (Los Angeles, California, 1971).
- 29 H. M. Colbert, "SANDYL: A Computer Code for Calculating Combined Photon-Electron Transport in Complex Systems," Sandia National Laboratories report SLL-74-0012 (Livermore, California, 1973).
- 30 J. A. Halbleib, Sr., "ACCEPT: A Three-Dimensional Electron/Photon Monte Carlo Code Using Combinational Geometry," Sandia National Laboratories report SAND 79-0415 (Albuquerque, New Mexico, 1979).
- 31 Richard L. Ford and Walter R. Nelson, "The EGS Code System: Computer Programs for the Monte Carlo Simulation of Electromagnetic Cascade Showers (Version 3)," Stanford Linear Accelerator Center report SLAC-210 (Stanford California, 1978).
- 32 J. A. Halbleib and T. A. Melhorn, "ITS: The Integrated TIGER Series of Coupled Electron/Photon Monte Carlo Transport Codes," Sandia National Laboratories report SAND 84-0573 (Albuquerque, New Mexico, November 1984).
- 33 H. H. Hsu, E. J. Dowdy, G. P. Estes, M. E. Hamm, M. C. Lucas, J. M. Mack, and C. E. Moss, "Efficiency of a Bismuth Germanate Scintillator: Comparison of Monte Carlo Calculations with Measurements," IEEE Trans. Nucl. Sci. NS-31 (1), 390 (February 1984).
- 34 Joseph M. Mack and Thomas M. Jordan, "Monte Carlo Simulation of Photon/Electron/Cerenkov Cascades in Generalized Geometry," Trans. Amer. Nucl. Soc. Annual Meeting (New Orleans, Louisiana, June 1984), p. 434.
- 35 Joseph M. Mack and Mahavir Jain, "Monte Carlo Simulation of Gas Cerenkov Detectors," IEEE Trans. Nucl. Sci. NS-32 (1), 668 (February 1985).
- 36 J. A. Halbleib, Sr., and W. H. Vandevender, "Coupled Electron Photon Collisional Transport in Externally Applied Electromagnetic Fields," J. Appl. Phys. 48 (6), 2312 (1977).
- 37 J. A. Halbleib, G. J. Lookwood, and G. H. Miller, "Optimization of Bremsstrahlung Energy Deposition," Sandia National Laboratories report SAND 76-5285 (Albuquerque, New Mexico, July 1976).
- 38 Joseph M. Mack, Los Alamos National Laboratory, personal communication, March 1985.
- 39 M. B. Emmett, "The MORSE Monte Carlo Radiation Transport Code System," Oak Ridge National Laboratory report ORNL-4972 (Oak Ridge, Tennessee, 1975).

- *0 M. Caro and J. Ligou, "Treatment of Scattering Anisotropy of Neutrons Through the Boltzmann-Fokker-Planck Equation," Nucl. Sci. Eng. 33, 242 (1983).
- *1 J. E. Morel, "Fokker-Planck Calculations Using Standard Discrete-Ordinates Code," Nucl. Sci. Eng. 79, 340 (1981).
- *2 T. M. Jordan, "An Adjoint Charged Particle Transport Method," Experimental and Mathematical Physics Consultants report EMP.L76.071 (Los Angeles, California, 1979).
- *3 Ronald Sagui, Thomas Jordan, Joseph Mack, George Radke, Jim Morel, Joseph Janni, "Computational Benchmarks for Electron Total Dose Shielding Methodology," (Computer Science Corporation, 1985), to be published.
- *4 Leonard J. Lorence, W. E. Nelson, and J. E. Morel, "Coupled Electron-Photon Transport Calculations Using the Method of Discrete-Ordinates," Los Alamos National Laboratory report LA-UR-85-692 (Los Alamos, New Mexico, 1985).
- *5 "HETC: A Monte Carlo High-Energy Nucleon-Meson Transport Code," Oak Ridge National Laboratory report CCC-178 (Oak Ridge, Tennessee, 1977).
- *6 T. M. Jordan, "TEMPER: A Time-Dependent, Multidimensional-Geometry Computer Program for Non-Linear Electron Transport Analysis," Applied Research Technology Corporation report ART-66 (Los Angeles, California 1972).
- *7 B. R. Wienke, "ESN: One-Dimensional S_n Transport Module for Electrons," J. Quant. Spec. and Rad. Trans. 28 (4), 311 (1982).
- *8 D. W. Forslund and J. U. Brackbill, "Magnetic Field Induced Surface Transport on Laser Irradiated Foils," Phys. Rev. Lett. 48 (23), 1614 (1982).

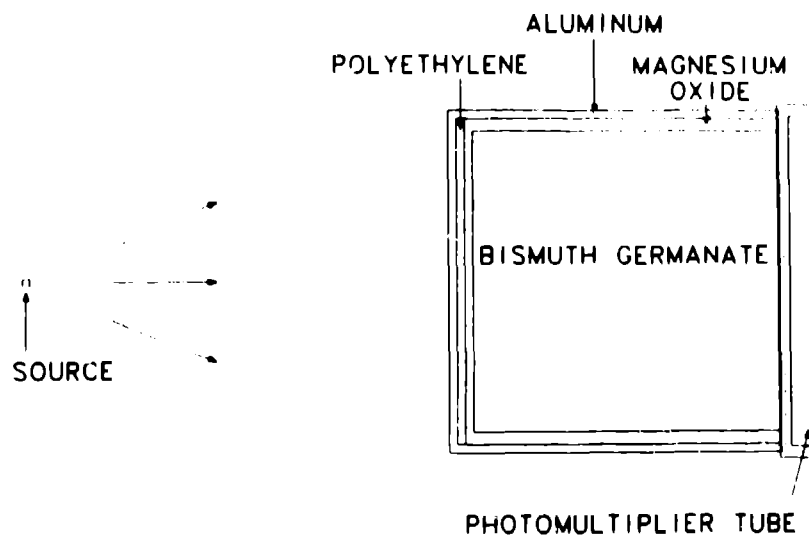


Fig. 1. BGO detector model geometry.

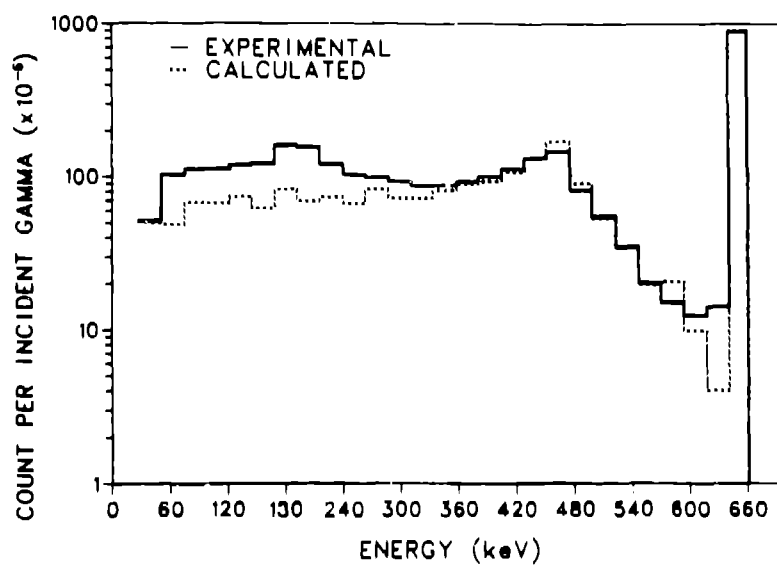


Fig. 2. Comparison of measured and calculated pulse-height distributions.

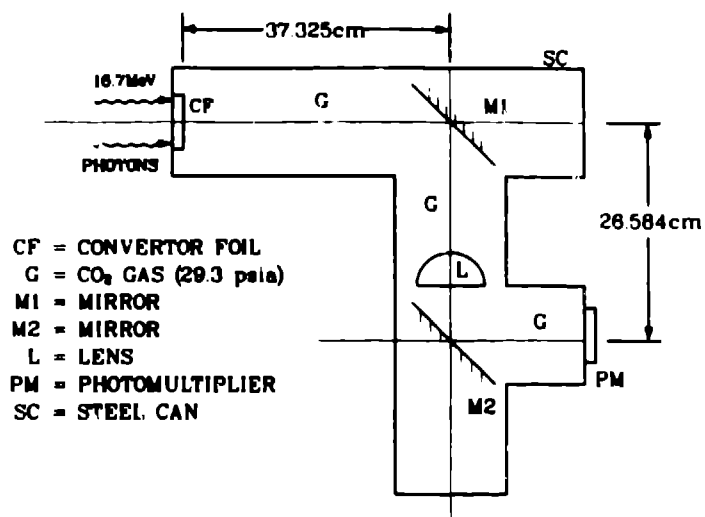


Fig. 3. Gas Cerenkov detector model geometry.

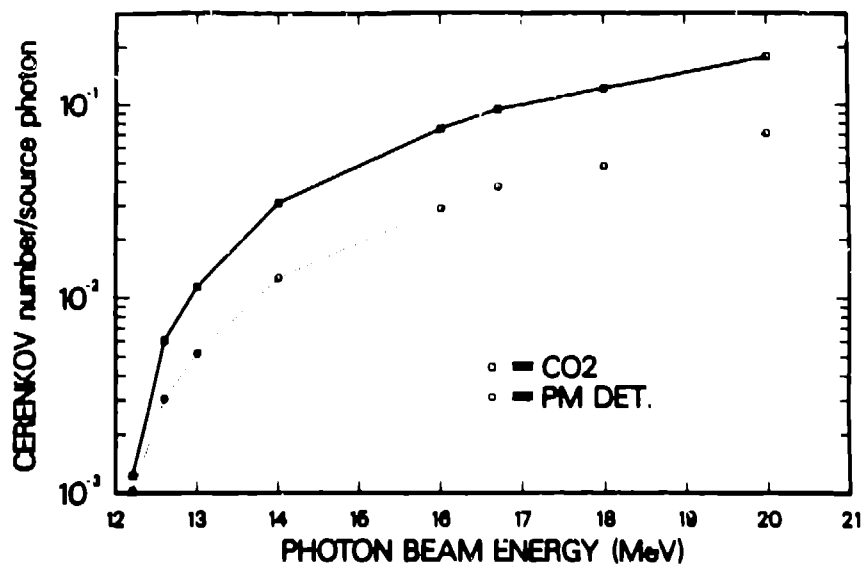


Fig. 4. Cerenkov production-threshold curves.

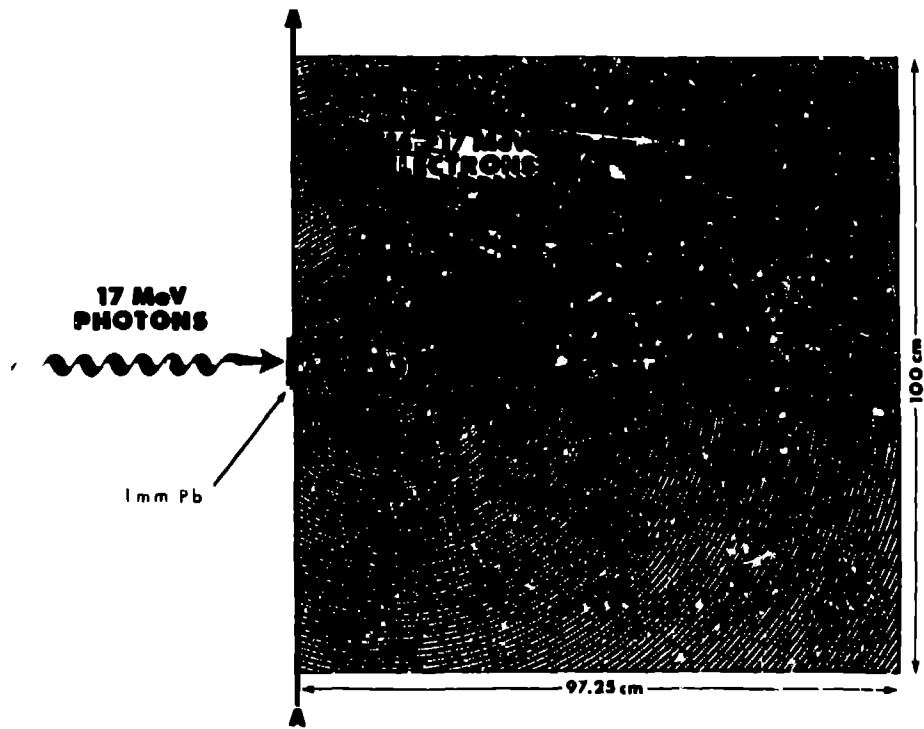


Fig. 5. Electron spectrometer model geometry.